

## NUMERICAL MODELLING OF THE AIRFOIL-VORTEX CLOUD INTERACTION

### Leandro Silva de Oliveira

Instituto de Engenharia Mecânica, UNIFEI, CP 50, Itajubá, Minas Gerais, 37500-903, Brasil  
e-mail: leandrosiol@yahoo.com.br

### Luiz Antonio Alcântara Pereira

Instituto de Engenharia Mecânica, UNIFEI, CP 50, Itajubá, Minas Gerais, 37500-903, Brasil  
e-mail: luizantp@unifei.edu.br

### Miguel Hiroo Hirata

FAT/UERJ  
Campus Regional de Resende  
Estrada Resende - Riachuelo, Resende, RJ  
e-mail: hirata@fat.uerj.com.br

### Nelson Manzanares Filho

Instituto de Engenharia Mecânica, UNIFEI, CP 50, Itajubá, Minas Gerais, 37500-903, Brasil  
e-mail: nelson@unifei.edu.br

**Abstract.** *The discrete vortex method is applied to simulate two-dimensional airfoil-vortex cloud interaction. In the numerical simulation a cloud of free vortices is used in order to simulate the vorticity, which is generated on the body surface, develops in the boundary layer and is carried out into the viscous wake. A second cloud of free vortex is generated next to the body; all the free vortices have the same strength. The dynamics of the wakes is computed using the convection-diffusion splitting algorithm, where the convection process is carried out with a Lagrangian second-order Adams-Bashforth time-marching scheme, and the diffusion process is simulated using the random walk scheme. The aerodynamics loads are computed using the integral equation derived from the pressure Poisson equation.*

**Keywords** *vortex methods, panels methods, airfoil-vortex interaction, aerodynamics loads.*

### 1. Introduction

The main goal of the research line, where this paper is inserted, consists of the analysis of the flow in a turbomachines.

This kind of flow is characterized by the interaction of the vortices generated by a rotor blade with the vortices generated by another blade of the same rotor. The viscous wake thus created interacts strongly with the casing surface.

It is also frequently found the situation where the rotor blades are immersed in a viscous wake – from now on referred to as a shear flow - generated by an upstream rotor (stator).

A cascade of identical airfoils represents a simple model, suitable for the analysis of the main characteristics of this flow. Many researchers using the potential flow theory have exploited this model. Recently, Alcântara Pereira et al (2004) extended the analysis including the viscous effects. In their work they used the Vortex Methods including an additional feature, the turbulence modelling, see Hirata (2000) and Alcântara Pereira et al (2002).

The above mentioned model considers the interaction of the flow generated by neighboring blades but does not take into account the presence of the casing surface, neither the oncoming vortex wake generated by an upstream stator or rotor. To analyze the influence of these aspects another simple model can be derived. This time one consider a single airfoil, near a ground plane, immersed in an upstream shear flow; this model is referred to as “the airfoil-vortex interaction in ground effect” – AVIG – and can be viewed as a combination of three interacting flows: airfoil-vortex interaction (AVI), airfoil-ground interaction (AGI), and vortex-ground interaction (VGI). A large number of papers on the unsteady, incompressible, two-dimensional AVI flow have been published. Within the context of the (two-dimensional) parallel AVI that occurs around helicopter rotors, known as blade-vortex interaction (BVI), Panaras (1987), Poling et al (1989) and Lee & Smith (1991), among others, have devised numerical models based on the inviscid discrete vortex method coupled with linearized potential flow theory. More elaborate numerical models have also been employed, such as those based on Euler (Srinivasan & McCroskey, 1993) and Navier-Stokes (Rai, 1987) mesh-based methods. Detailed experimental investigations on the aerodynamics of parallel BVI have been performed by Seath et al (1989), Straus et al (1990) and Chen & Chang (1997). See the review articles of McCune & Tavares (1993) and Mook & Dong (1994) for additional references on unsteady, incompressible flows over airfoils and the numerical simulation of wakes and BVI.

Chacaltana et al (1995) analyze the flow around a thin airfoil immersed in a shear flow, in presence of a ground plane. The authors use the potential flow theory and taking into account the fact that the airfoil is thin were able to derive a simple algorithm. In this paper, the shear flow was simulated by a single moving free vortex.

Fonseca et al (1997, 2003) in a series of two papers applied a numerical, inviscid, vortex method to simulate the unsteady, two-dimensional and incompressible flow that occurs during a parallel blade-vortex interaction in ground effect. A panel method was used to discretize the airfoil bound vorticity, where each panel has a linear and piecewise-continuous distribution of vorticity. The impermeability condition was enforced on the airfoil contour, but the no-slip condition is not. The Kutta condition was imposed through the continuity of the pressure field at the airfoil trailing edge, which, combined with the condition that the circulation in the whole flow must be conserved, provides a model for the vorticity generation at the trailing edge. Thus the viscous wake was modeled by potential vortices shed into the flow at the trailing edge and the oncoming shear flow was modeled by a single potential vortex that interacts with the airfoil and its wake.

Medeiros et al (2002) use the Vortex Methods to simulate the flow around an airfoil immersed in a shear flow. This paper presents two new features. First, the shear flow is more complex than the previous one and it is represented by a cloud of vortices with a viscous core (Lamb vortices). The second new feature is related to the viscous wake that was simulated by another cloud of free vortices generated on the whole airfoil surface; the two vortex clouds strongly interact near and downstream the airfoil.

In the present paper, the Vortex Methods is employed to simulate the airfoil-vortex cloud interaction, see Fig. (1); the ground effect is not included. The main feature of the paper is the oncoming shear flow that has two important characteristics. The first is that the shear flow is continuously generated is a plane perpendicular to the main flow, a feature not found in any of the previous paper, and the second characteristic is the possibility of having a time variation of the vorticity carried out by this shearing flow. It is believed that with these two features the shear flow due to the upstream rotor could be simulated in a more realistic way; after all, the rotor always moves in relation to the upstream rotor or stator.

To simulate the oncoming shear flow, a cloud of free Lamb vortices is generated next to the body. For this one can imagine a row of vortex generating points that are aligned in a previously fixed position. This row of vortices moves in a direction perpendicular to the main flow at a pre-set velocity  $V$ , see Fig. (1).

As mentioned, the model is analyzed using the Vortex Methods which is a meshless numerical method or a particle method. In this method, the vorticity in the fluid region is numerically simulated using a cloud of discrete vortices with a viscous core (Lamb vortex). To simulate the vorticity at the solid surfaces, nascent vortices are generated there at each time step of the simulation. In order to take care of the convection and the diffusion of the vorticity one make use of the convection-diffusion splitting algorithm; accordingly the convection of the vortices in the cloud is carried out independently of the diffusion for each time step of the simulation. The convection process is carried out with the Adams-Bashforth time-marching scheme and the diffusion process is simulated using the random walk method. This is in essence the foundation of the Vortex Methods (e.g. references Chorin, 1973; Sarpkaya, 1989; Sethian, 1991; Kamemoto, 1994; Lewis, 1999; Ogami, 2001 and Hirata, 2000). Please note that with the lagrangian formulation a grid for the spatial discretization of the fluid region is not necessary. Thus, special care to handle numerical instabilities associated to high Reynolds numbers is not needed. Also, the attention is only focused on the regions of high activities, which are the regions containing vorticity; on the contrary, Eulerian schemes consider the entire domain independent of the fact that there are sub-regions where less important, if any, flow activity can be found. With the Lagrangian tracking of the vortices, one need not take into account the far away boundary conditions. This is of important in the wake regions (which is not negligible in the flows of present interest) where turbulence activities are intense and unknown, a priori.

## 2. Formulation of the Physical Problem

Consider the incompressible fluid flow of a Newtonian fluid around an airfoil in an unbounded two-dimensional region. Figure (1) shows the incident flow, defined by free stream speed  $U$  and the domain  $\Omega$  with boundary  $S = S_1 \cup S_2$ ,  $S_1$  being the body surface and  $S_2$  the far away boundary. A cloud of free vortices is generated, next to the body, in a row of points, which move in the  $y$  direction with constant speed  $V$ ; at every time step a new vortex is generated in each of the points of the row. All the vortices of this cloud have the same strength  $\Delta\Gamma$  (negative or positive) in this paper.

The viscous and incompressible fluid flow is governed by the continuity and the Navier-Stokes equations, which can be written in the form

$$\nabla \cdot \mathbf{u} = 0 \quad (1)$$

$$\frac{\partial \mathbf{u}}{\partial t} + \mathbf{u} \cdot \nabla \mathbf{u} = -\nabla p + \frac{1}{\text{Re}} \nabla^2 \mathbf{u}. \quad (2)$$

In the equations above  $\mathbf{u}$  is the velocity vector field and  $p$  is the pressure. All the quantities in Eqs. (1), (2) and the equations bellow are nondimensionalized by  $U$  and  $b$  (the airfoil chord). The Reynolds number is defined by

$$Re = \frac{bU}{\nu} \quad (2a)$$

where  $\nu$  is the fluid kinematics viscosity coefficient. The dimensionless time is  $b/U$ .

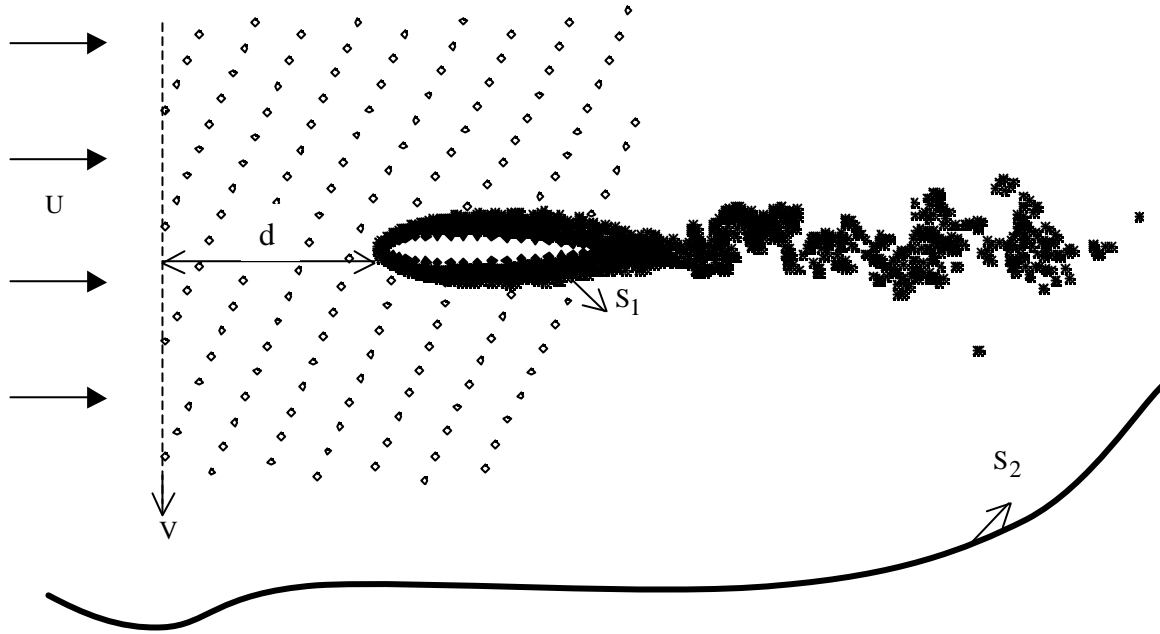


Figure 1. Definitions.

The impenetrability and no-slip conditions on the body surface are written as

$$\mathbf{u}_n = \mathbf{u} \cdot \mathbf{e}_n = 0 \quad (3a)$$

$$\mathbf{u}_\tau = \mathbf{u} \cdot \mathbf{e}_\tau = 0 \quad (3b)$$

$\mathbf{e}_n$  and  $\mathbf{e}_\tau$  being, respectively, the unit normal and tangential vectors. One assumes that, far away, the perturbation caused by the body fades as

$$|\mathbf{u}| \rightarrow 1 \text{ at } S_2. \quad (3c)$$

The dynamics of the fluid motion, governed by the boundary-value problem (1), (2) and (3), can be alternatively studied by taking the curl of Eq. (2), obtaining the well-known 2-D vorticity transport equation

$$\frac{\partial \omega}{\partial t} + \mathbf{u} \cdot \nabla \omega = \frac{1}{Re} \nabla^2 \omega \quad (4)$$

in which  $\omega$  is the only non-zero component of the vorticity vector.

### 3. Numerical Simulation

According to the convection-diffusion splitting algorithm (Chorin, 1973) it is assumed that in the same time increment the convection and the diffusion of the vorticity can be independently handled and are governed by

$$\frac{\partial \omega}{\partial t} + \mathbf{u} \cdot \nabla \omega = 0 \quad (5)$$

$$\frac{\partial \omega}{\partial t} = \frac{1}{\text{Re}} \nabla^2 \omega. \quad (6)$$

Convection is governed by Eq. (5) and the velocity field is given by

$$\mathbf{u} - i\mathbf{v} = 1 + \frac{i}{2\pi} \sum_{n=1}^M \gamma(S_n) \int_{\Delta S_n} \frac{d}{dz} \ln(z - \zeta) d\zeta + \frac{i}{2\pi} \sum_{n=1}^N \Delta \Gamma_n K(x - x_n). \quad (7)$$

Here,  $u$  and  $v$  are the  $x$  and  $y$  components of the velocity vector  $\mathbf{u}$  and  $i = \sqrt{-1}$ . The first term in the right hand side is the contribution of the incident flow; the summation of  $M$  integral terms comes from the vorticity panels used to simulate the body surface. The second summation is associated to the velocity induced by the cloud of  $N$  free vortices; it represents the vortex-vortex interactions.

In the second summation of Eq. (7), the Lamb vortex kernel is used in order to avoid the singularity present in the potential vortex kernel. The expression of this kernel can be easily derived from the expression for the induced velocity of the  $k$ th vortex with strength  $\Delta \Gamma_k$  in the circumferential direction  $\mathbf{u}_{\theta_k}$ , (Mustto et al, 1998):

$$\mathbf{u}_{\theta_k} = \frac{\Delta \Gamma_k}{2\pi r} \left\{ 1 - \exp \left[ -5.02572 \left( -\frac{r}{\sigma_0} \right)^2 \right] \right\} \quad (8)$$

where  $\sigma_0$  is core radius of the Lamb vortex and  $r$  is the distance from the core center.

Each vortex particle distributed in the flow field is followed during numerical simulation according to the Adams-Bashforth second-order formula (Ferziger, 1981)

$$z(t + \Delta t) = z(t) + [1.5\mathbf{u}(t) - 0.5\mathbf{u}(t - \Delta t)]\Delta t + \xi \quad (9)$$

in which  $z$  is the position of a particle,  $\Delta t$  is the time increment and  $\xi$  is the random walk displacement. According to Lewis (1991), the random walk displacement is given by

$$\xi = \sqrt{4\beta \Delta t \ln \left( \frac{1}{P} \right)} [\cos(2\pi Q) + i \sin(2\pi Q)] \quad (10)$$

where  $\beta = \text{Re}^{-1}$ ;  $P$  and  $Q$  are random numbers between 0.0 and 1.0.

The pressure calculation starts with the Bernoulli function, defined by Uhlman (1992) as

$$Y = p + \frac{\mathbf{u}^2}{2}, \quad \mathbf{u} = |\mathbf{u}|. \quad (11)$$

Kamemoto (1993) used the same function and starting from the Navier-Stokes equations was able to write a Poisson equation for the pressure. This equation was solved using a finite difference scheme. Here the same Poisson equation was derived and its solution was obtained through the following integral formulation (Shintani & Akamatsu, 1994)

$$H \bar{Y}_i - \int_{S_1} \bar{Y} \nabla G_i \cdot \mathbf{e}_n dS = \iint_{\Omega} \nabla G_i \cdot (\mathbf{u} \times \omega) d\Omega - \frac{1}{\text{Re}} \int_{S_1} (\nabla G_i \times \omega) \cdot \mathbf{e}_n dS \quad (12)$$

where  $H$  is 1.0 inside the flow (at domain  $\Omega$ ) and is 0.5 on the boundary  $S_1$ .  $G_i = (1/2\pi) \log R^{-1}$  is the fundamental solution of Laplace equation,  $R$  being the distance from  $i$ th vortex element to the field point.

It is worth to observe that this formulation is specially suited for a Lagrangian scheme because it utilizes the velocity and vorticity field defined at the position of the vortices in the cloud. Therefore it does not require any additional calculation at mesh points. Numerically, Eq. (12) is solved by mean of a set of simultaneous equations for pressure  $Y_i$ .

#### 4. Discussion and Results

The numerical simulations were restricted to the simple situation of a symmetrical airfoil, NACA 0012, at zero incidence. The Reynolds number was set equal to  $Re=10^6$ . The airfoil surface was represented by fifty ( $M=50$ ) straight-line segment panels on which vorticity with constant density were distributed. In each time step the nascent vortices were placed into the cloud through a displacement  $\epsilon=\sigma_0=0.03b$  normal to the panels. The simulations were performed up to 400 time steps with magnitude  $\Delta t=0.05$ . The aerodynamic forces computations starts at  $t=10$ .

The results presented in this section were obtained for three cases. First, we remove the shear flow and simulate a NACA 0012 airfoil immersed in a uniform flow. Figure (2) shows that the lift coefficient oscillates around zero. The differences encountered in the comparison of the numerical result with the expected result are attributed mainly to the inherent three-dimensionality of the real flow for such a value of the Reynolds number, which is not modeled in the simulation.

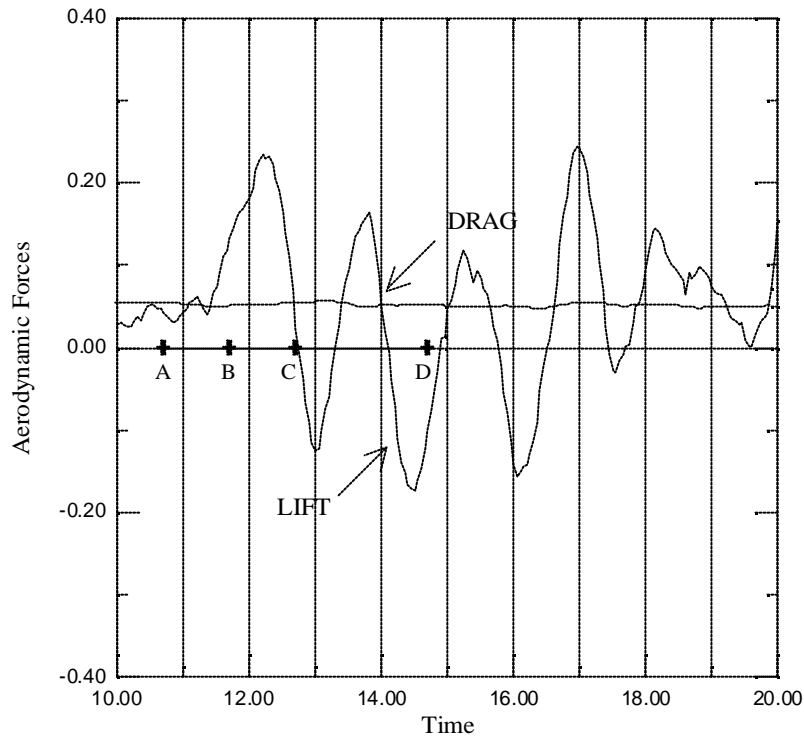


Figure 2. NACA 0012 airfoil: Time development of the lift coefficient at Reynolds number to  $Re=10^6$ .

Second, we simulate the interaction of a NACA 0012 airfoil with a shear flow simulated by a second cloud of free vortices (generated at the row of moving points) that passes over the airfoil. Each vortex generated at row of points has dimensionless strength  $\Delta\Gamma=+ 0.001$ . The row with length  $2b$  and  $V=0.065U$  was located at distance  $d=b$ , see Fig. (1). The distance between two points of the row was equal to  $0.5b$ . To avoid the influence of numerical transients, we start the simulation with the airfoil in an uniform flow without shear and we insert the shear flow only after the numerical simulation has been established ( $t=10$ ).

Figure (3) shows the time development of the lift and drag coefficient for an airfoil at zero incidence but immersed in a shear flow.

In the numerical simulation with shear flow (simulated with a cloud of positive vortices,  $\Delta\Gamma=+ 0.001$ ), we follow a free vortex generated on it. We selected a vortex generated on the x-axis. In Fig. (4), the positions of this free vortex at  $t=10.8$ ,  $t=11.8$ ,  $t=12.8$  and  $t=13.8$  are indicated by points A, B, C and D, respectively; as can be observed this vortex follows a straight line path until a point B close to the airfoil leading edge. At this point the interaction with the body and with the vortices generated (boundary layer) on it becomes visible and the vortex follows a path along the lower side of the airfoil, drifting away from it. At point C, the interaction with the airfoil wake is strong and finally at point D the vortex can be already considered as part of the airfoil wake. After this, one have a full interaction of the two vortex cloud and the simulation goes on. This picture becomes clearer observing the Fig. (5), which shows the two vortex cloud as they interact. For a longer numerical simulation new features can be observed as the strong vortex structures detaches from the body neighborhood from time to time. We are still analyzing such a complex phenomena and do not have yet a clear picture

As the airfoil is thin (slender body), the interactions of the vortices used to represent the shear flow with those representing the airfoil wake is restricted to a narrow region that extend more or less a half airfoil length up and down

the  $x$ -axis. Nevertheless, the results of these interactions are dramatically strong on the flow characteristics. For example, the time evolution of the lift coefficient is affected by the presence of the shear flow as can be devised comparing behavior showed in Fig. (2) with the one showed in Fig. (3).

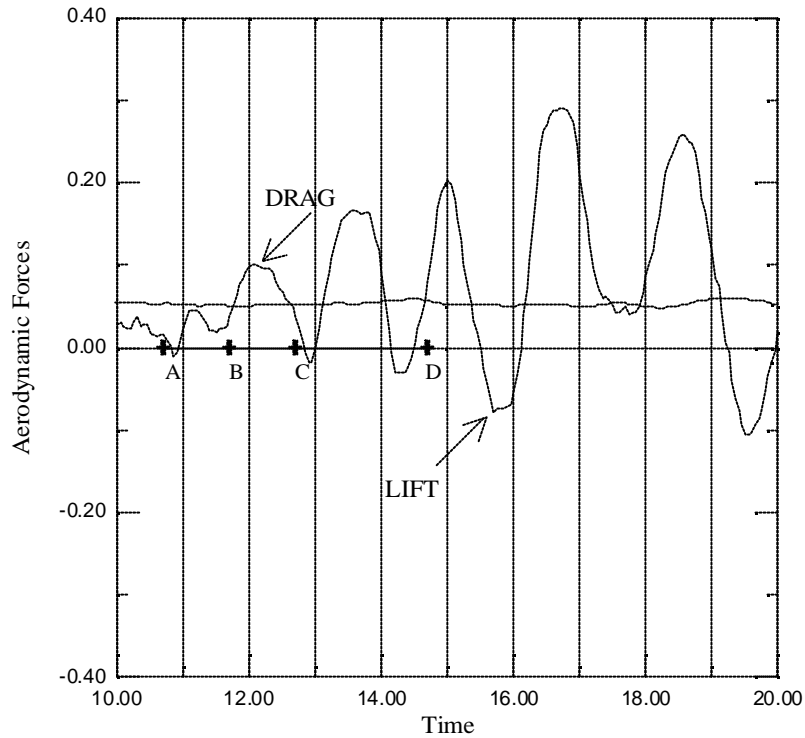


Figure 3. NACA 0012 airfoil in a shear flow simulated with positive vortices ( $\Delta\Gamma=+ 0.001$ ). Time development of the lift coefficient at Reynolds number to  $Re=10^6$ .

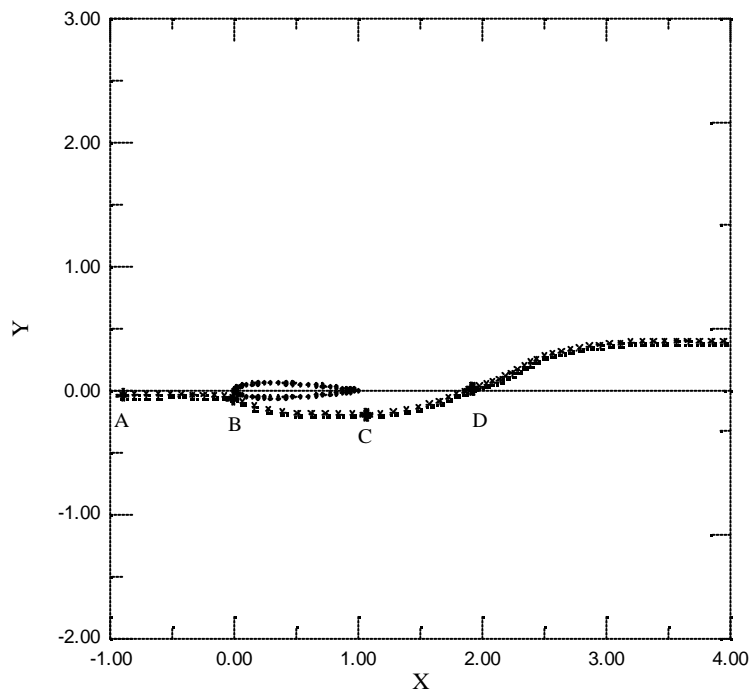


Figure 4. Drift path of a positive vortex that belongs to the cloud used to simulate the shear flow.

As the vortex cloud used to simulate the shear flow is generated close to the airfoil, its influence can be observed right away, even before the front edge of the vortex cloud reaches the body. In fact, before the time  $t=12$  (point B) of

the simulation one can observe a decrease of the lift coefficient. From then on, the interaction is strong and the lift coefficient does not assume a negative value until time  $t=14.5$  when it oscillates assuming a still small negative value at time  $t=15.5$ . From time  $t=16$  of the simulation the lift oscillates but becomes highly positive until time  $t=19$ . From then it changes its behavior probably due to the detachment of a strong vortex structure from the airfoil neighborhood.

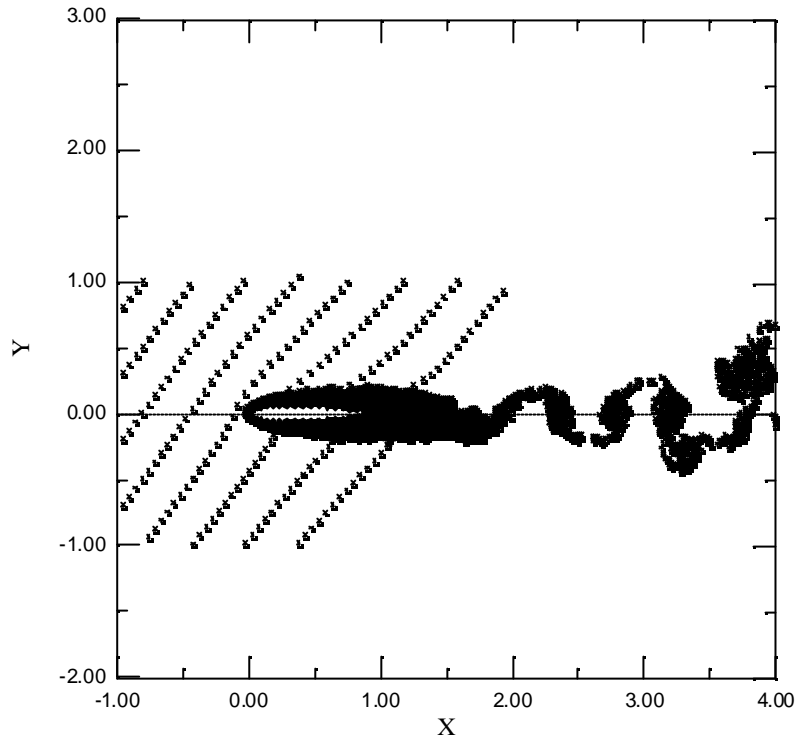


Figure 5. NACA 0012 airfoil: Vortex wake structure at  $t=12.8$ , with shear flow simulated with positive vortices.

Figure (6) shows the lift and drag coefficient evolution for the flow around the same airfoil immersed in a shear flow, this time simulated with a cloud of negative vortices ( $\Delta\Gamma = -0.001$ ).

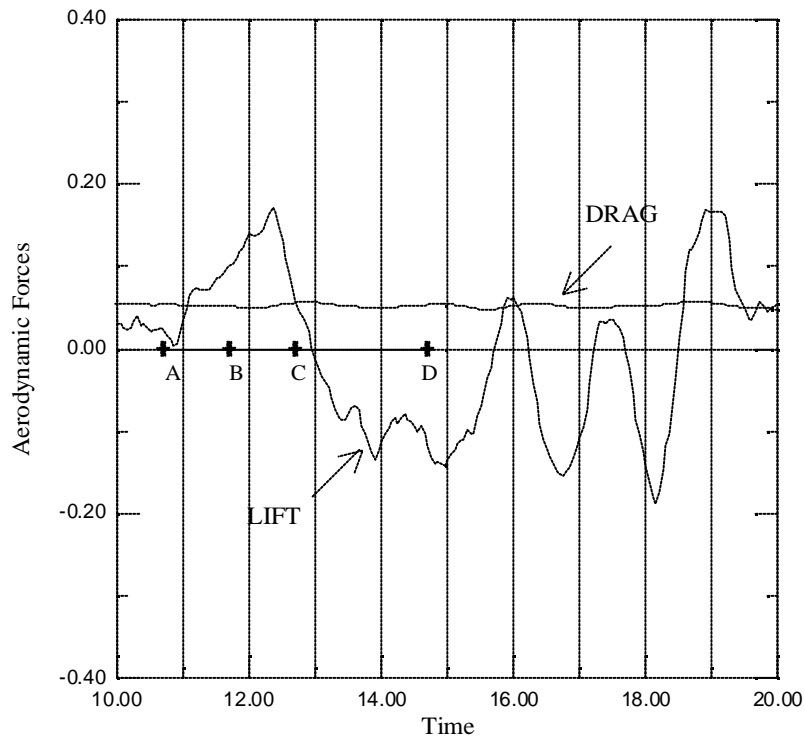


Figure 6. NACA 0012 airfoil in a shear flow simulated with negative vortices ( $\Delta\Gamma = -0.001$ ). Time development of the lift coefficient at Reynolds number to  $Re=10^6$ .

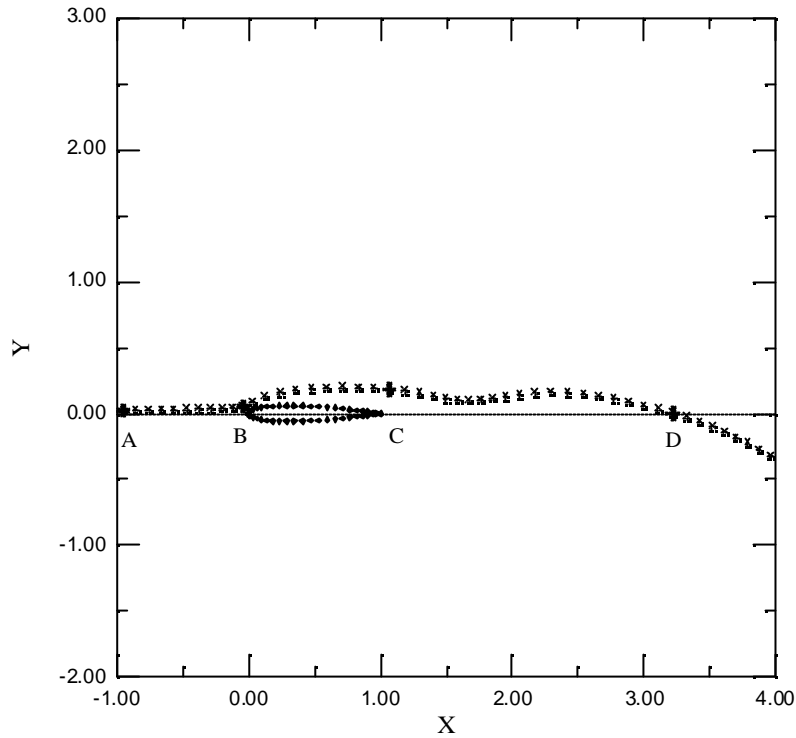


Figure 7. Drift path of a negative vortex that belongs to the cloud used to simulate the shear flow.

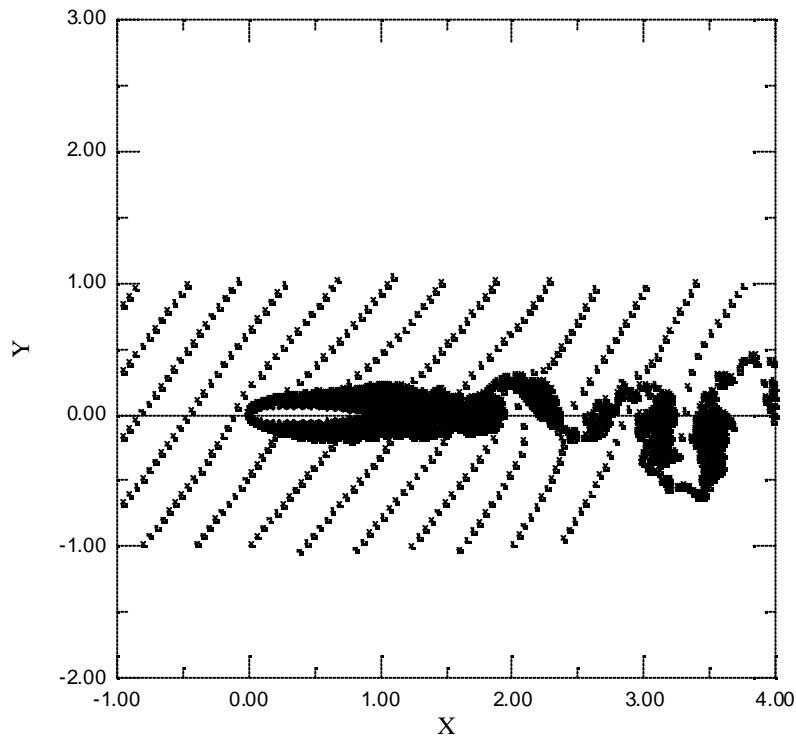


Figure 8. NACA 0012 airfoil: Vortex wake structure at  $t=14.7$ , with shear flow simulated with negative vortices.

Figure (7) shows the drift path of a negative vortex of the cloud used to simulate the shear flow; the general features of this path are the same as the one showed in Fig. (4), obviously taking into account the fact that this time de vorticity is negative. Figure (8) shows the instantaneous wake for the time  $t=14.7$ . In this figure the time simulation was longer than the one of Fig.(5) which allows one to observe how the vortices from different clouds interacts in the wake.



It is also obvious that a more dense vortex cloud is necessary to simulate the shearing flow; this will be an important point to take into consideration in future work.

The comparison of the time evolution of the lift coefficient for a shear free oncoming flow, and the lift coefficient for the shearing flows shows some interesting features. While the front end of the shearing cloud is passing by the airfoil (which can be considered as a transient regime in some sense) the effect on the lift due to the interactions is to flatten the maximum values; this can probably be explained by considering the change of leading edge stagnation point position. Once the front end reaches the wake, interactions which dramatically changes the lift behavior can be observed; with the positive shearing flow the lift is almost positive, while it is almost always a negative value for the negative shearing flow.

## **5. Conclusions**

The main objective of the work was to implement the algorithm and to get some insight into the potentialities of the model developed; this was accomplished since the results show that the behavior of the quantities of interest is the expected one.

The results also allowed one to get an insight on the appropriate parameters needed for the numerical simulation, as for example, the vortex density of the shearing cloud, the value of the velocity  $V$ , etc. It is considered of importance to determine the generating law for vortices of the shearing flow.

Finally one should observe that the algorithm used to generate the presented results can be easily adapted for the analysis of the flow in presence of a ground plane. The sub-grid turbulence modelling is of significant importance for the numerical simulation. The results of this analysis, taking into account the sub-grid turbulence modelling, are being generated and will be presented in due time, elsewhere.

## **6. Acknowledgement**

The authors would like to acknowledge FAPEMIG (Processes TEC-00025/02 and TEC-00063/02) and CNPq for the financial support during the time of this project.

## **7. References**

- Alcântara Pereira, L.A., Hirata, M.H. and Manzaneres Filho, N. 2004, "Wake and Aerodynamics Loads in Multiple Bodies – Application to Turbomachinery Blade Rows", *J. Wind Eng. Ind Aerodyn.*, 92, pp. 477-491.
- Alcântara Pereira, L.A., Ricci, J.E.R., Hirata, M.H. and Silveira-Neto, A., 2002, "Simulation of Vortex-Shedding Flow about a Circular Cylinder with Turbulence Modeling", *Intern'l Society of CFD*, vol. 11, no. 3, October, pp. 315-322.
- Chacaltana, J.T.A., Bodstein, G.C. R. and Hirata, M.H., 1995, "Analytical Study of the Time-Dependent 2-D Interaction of a Thin Airfoil and a Vortex in the Presence of a Ground-Plane", *Proceedings of XIII Brazilian Congress of Mechanical Engineering, XIII COBEM*, Belo Horizonte, MG, Brazil.
- Chen, J.M. and Chang, D.M., 1997, "Unsteady Pressure Measurements for Parallel Vortex-Airfoil Interaction at Low Speed", *Journal of Aircraft*, vol. 34, no. 3, pp. 330-336.
- Chorin, A.J., 1973, "Numerical Study of Slightly Viscous Flow", *Journal of Fluid Mechanics*, vol. 57, pp. 785-796.
- Ferziger, J.H., 1981, "Numerical Methods for Engineering Application", John Wiley & Sons, Inc.
- Fonseca, G.F., Bodstein, G.C.R. and Hirata, M.H., 1997, "A Numerical Inviscid Vortex Model Applied to Parallel Blade-Vortex Interaction", *Journal of the Brazilian Society of Mechanical Sciences*, vol. 19, no. 3, pp. 341-356.
- Fonseca, G.F., Bodstein, G.C.R. and Hirata, M.H., 2003, "Numerical Simulation of Inviscid Incompressible Two-Dimensional Airfoil-Vortex Interaction in Ground Effect", *Journal of Aircraft*, vol. 40, no. 4, July-August, pp. 653-661.
- Hirata, M.H., 2000, "O Método de Vórtices com Modelagem de Turbulência", *Palestra Oficial, proferida no Congresso Norte-Nordeste de Engenharia Mecânica – CONEN 2000*, Natal, RN, Brasil.
- Kamemoto, K., 1993, "Procedure to Estimate Unstead Pressure Distribution for Vortex Method" (In Japanese), *Trans. Jpn. Soc. Mech. Eng.*, vol. 59, no. 568 B, pp. 3708-3713.
- Kamemoto, K., 1994, "Development of the Vortex Methods for Grid-Free Lagrangian Direct Numerical Simulation", *Proc. Third JSME-KSME*, Sendai, Japan, pp. 542-547.
- Lee, D.J. and Smith, C.A., 1991, "Effect of Vortex Core Distortion on Blade-Vortex Interaction", *A.I.A.A. Journal*, vol. 29, no. 9, pp. 1355-1362.
- Lewis, R. I., 1991, "Vortex Element Method for Fluid Dynamic Analysis of Engineering Systems", Cambridge Univ. Press, Cambridge, England, U.K..
- Lewis, R.I., 1999, "Vortex Element Methods, The Most Natural Approach to Flow Simulation - A Review of Methodology with Applications", *Proceedings of 1<sup>st</sup> Int. Conference on Vortex Methods*, Kobe, Nov. 4-5, pp. 1-15.
- McCune, J.E. and Tavares, T.S., 1993, "Perspective: Unsteady Wing Theory – The Karman/Sears Legacy", *Journal of Fluids Engineering*, vol. 115, Dec., pp. 548-560.

- Medeiros, E.N., Araújo, Z.A., Hirata, M.H. and Ricci, J.E.R., 2002, “Simulação Numérica da Interação entre uma Nuvem de Vórtices e um Aerofólio”, II National Congress of Mechanical Engineering, CONEM 2002, João Pessoa, PB, Brasil.
- Mustto, A.A., Hirata, M.H. and Bodstein, G.C.R., 1998, “Discrete Vortex Method Simulation of the Flow Around a Circular Cylinder with and without Rotation”, A.I.A.A. Paper 98-2409, Proceedings of the 16<sup>th</sup> A.I.A.A. Applied Aerodynamics Conference, Albuquerque, NM, USA, June.
- Mook, D.T. and Dong, B., 1994, “Perspective: Numerical Simulations of Wakes and Blade-Vortex Interaction”, *Journal of Fluids Engineering*, vol. 116, March, pp. 5-21.
- Ogami, Y., 2001, “Simulation of Heat-Fluid Motion by the Vortex Method”, *J.S.M.E. International Journal, Series B*, vol. 44, no. 4, pp. 513-519.
- Panaras, A.G., 1987, “Numerical Modeling of the Vortex/Airfoil Interaction”, *A.I.A.A. Journal*, vol. 25, no. 1, pp. 5-11.
- Poling, D.R., Dadone, L. and Telionis, D.P., 1989, “Blade-Vortex Interaction”, *A.I.A.A. Journal*, vol. 27, no. 6, pp. 694-699.
- Rai, M.M., 1987, “Navier-Stokes Simulations of Blade-Vortex Interaction Using High-Order Accurate Upwind Schemes”, A.I.A.A. Paper 87-0543, November.
- Sarpkaya, T., 1989, “Computational Methods with Vortices - The 1988 Freeman Scholar Lecture”, *Journal of Fluids Engineering*, vol. 111, pp. 5-52.
- Seath, D.D., Kim, J.M. and Wilson, D.R., 1989, “Investigation of Parallel Blade-Vortex Interaction at Low Speed”, *Journal of Aircraft*, vol. 26, no. 4, pp. 328-333.
- Sethian, J.I., 1991, “A Brief Overview of Vortex Method, Vortex Methods and Vortex Motion”, SIAM. Philadelphia, pp. 1-32.
- Shintani, M. and Akamatsu, T., 1994, “Investigation of Two Dimensional Discrete Vortex Method with Viscous Diffusion Model”, *Computational Fluid Dynamics Journal*, vol. 3, no. 2, pp. 237-254.
- Srinivasan, G.R. and McCroskey, W.J., 1993, “Euler Calculations of Unsteady Interaction of Advancing Rotor with a Line Vortex”, *A.I.A.A. Journal*, vol. 31, no. 9, pp. 1659-1666.
- Straus, J., Renzoni, P. and Mayle, R.E., 1990, “Airfoil Pressure Measurement During a Blade Vortex Interaction and a Comparison with Theory”, *A.I.A.A. Journal*, vol. 28, no. 2, pp. 222-228.
- Uhlman, J.S., 1992, “An Integral Equation Formulation of the Equation of an Incompressible Fluid”, Naval Undersea Warfare Center, T.R. 10-086.